Electronic Supplementary Material (ESI) for Materials Horizons.

A self-healing polymerized-ionic-liquid-based polymer electrolyte enables long lifespan and dendrite-free solid-state Li metal batteries at room temperature

Xiujing Lin[a], Shiyuan Xu[a], Yuqi Tong[a], Xinshuang Liu[a], Zeyu Liu[a], Pan Li [a], Ruiqing Liu[a], Xiaomiao Feng[a], Li Shi[a]*, Yanwen Ma*[a, b]

[a]*Key Laboratory for Organic Electronics and Information Displays (KLOEID) & Institute of Advanced Materials (IAM), Jiangsu Key Laboratory for Biosensors, Jiangsu National Synergetic Innovation Center for Advanced Materials (SICAM), Nanjing University of Posts and Telecommunications, Nanjing, Jiangsu 210023, China*

[b]*Suzhou Vocational Institute of Industrial Technology, 1 Zhineng Avenue, Suzhou International Education Park, Suzhou 215104, China.*

Corresponding Author

*E-mail address: iamlshi@njupt.edu.cn

*E-mail address: iamywma@njupt.edu.cn

Experimental section

Synthesis of EMEImBr monomer (ionic liquid monomer): According to previous work, [1-2] the synthesis of EMEImBr monomer is displayed in Scheme 1. Firstly, a solution containing 2-bromoethanol and triethylamine in tetrahydrofuran (THF) was prepared. Methacryloyl chloride in THF solution was added dropwise at 0 °C under inert N_2 atmosphere. The obtained mixture was stirred for 48 h at ambient temperature, followed by filtrate and washed thoroughly with deionized H_2O. The resultant outcome was dried with anhydrous $MgSO_4$ and placed in vacuum to remove the solvent. The product 2-bromoethyl methacrylate was achieved. N-ethylimidazole was mixed with 2-bromoethyl methacrylate, along with a minute amount of phenothiazine. After stirring for 120 h at 60 °C under nitrogen (N_2) gas atmosphere, the reaction mixture was subsequently diluted with methylene chloride (200 ml) and filtered through a silica gel column.

Polymerization: The polymerization of monomers was proceeded at 65 °C under N_2 atmosphere with AIBN as initiators. After polymerization, the solution was filtered and washed with methyl alcohol for several times, followed by vacuum drying at 60 °C for overnight. ^{1}H NMR (400 MHz, DMSO-d_6, δ): 9.42 (s, 1H), 7.87 (d, 2H), 6.04 (s, 1H), 5.72 (s, 1H), 4.55 (t, 2H), 4.44 (t, 2H), 4.24 (q, 2H), 1.86 (s, 3H), 1.42 (t, 3H).

For the anion exchange, the above poly(ionic liquid) (PEMEImBr, 100 mg) was dispersed in 100 ml deionized water containing LiTFSI salt (200 mg, 99.95% from Sigma-Aldrich). After stirring for 48 h at room temperature, the precipitate was collected by filtration and kept vacuum drying at 60 °C for overnight to remove the residual moisture. The obtained mixture was denoted as PEMEImTFSI.

Fabrication of the solid electrolytes: The precursor ink was prepared by mixing 50 mg PEMEImTFSI and 28.7 mg LiTFSI in NMP solution with the assistance of ultrasound to obtain a

homogenous suspension. Subsequently, the mixture was directly dispensed onto Li anodes, followed by drying in vacuum at 80 °C for overnight to evaporate the NMP solvent. The as-obtained electrolytes was adherent to Li anodes, which was abbreviated as Li/PIL. Finally, a series of Li/PIL samples with different PIL thickness were synthesized by adjusting the amounts of the suspension above.

Characterizations: The morphologies of membranes and cycled Li anodes were characterized by a field emission scanning electron microscope (FESEM, Hitachi S4800). TGA evaluation (STA-449F3, Netzsch) was utilized to investigate the thermal stability of the membrane at 5 °C min^{-1} under argon atmosphere. The XPS experiments were conducted on a KRATOS Axis Supra to detect the chemical constituent of SEI layer and explore the chemical durability of membranes. The EMEImBr monomer polymerization was measured by the Fourier transform infrared spectra (FTIR, PE-Specturm Two), and the corresponding molecular weight distribution was studied by Agilent PL-GPC50 gel permeation chromatography (GPC). ^{1}H NMR and ^{13}C NMR were conducted on a Bruker Avance III spectrometer at 400 MHz with deuterated DMSO as a solvent.

Electrochemical characterizations: The galvanostatic charge/discharge measurements were carried out on CT2001A Land instrument (Wuhan LAND Electronics Co, Ltd) in the potential range of 2.5-4.3 V at various rates. The $LiFePO_4$ (LFP) cathode slurry comprises of LFP, Super P and PVDF at a mass ratio of 8:1:1 with N-methyl-2-pyrrolidone (NMP) as the disperse medium, which was blade-casted on precleaned Al foil and heated at 80 °C for 12 h in vacuum. The mass loading of the cathode is 2.6-3.0 mg cm^{-2} by getting rid of the weight of collectors. The Li|LFP batteries were fabricated by stacking the LFP cathode on the other side of PIL membrane in an argon-filled glove box with the content of moisture and O_2 lower than 10 ppm. The symmetric batteries were assembled with the same procedures by replacing the LFP cathode with Li foil,

which were subjected to Li plating/stripping processes at current densities of 0.01, 0.02, 0.05, 0.1 and 0.2 mA cm^{-2}, respectively. GITT test was conducted at 0.1 C with 0.5 h charge/discharge interval following 0.5 h relaxation.

The linear sweep voltammetry (LSV), electrochemical impedance spectroscopy (EIS) measurements and lithium transference number were studied on a BioLogic VMP3 electrochemical workstation. The electrochemical stability of the synthesized PIL electrolyte was carried out on a Li|PIL|stainless steel battery via LSV method at a sweep rate of 0.5 mV s^{-1} in the potential range from OCV to 6 V. The lithium transference number (t_{Li}^{+}) was determined on a Li|PIL|Li battery under a polarization potential of 10 mV (ΔV) until a steady status was reached. The initial (I_0) and steady state current (I_s) were collected. The interfacial resistances before (R_1^0) and after (R_1^s) the polarization scans were likewise taken. The t_{Li}^{+} was estimated according to the equation below:

$$t_{Li}^{+} = \frac{I_s\left[\Delta V - I_0 R_1^0\right]}{I_0\left[\Delta V - I_s R_1^s\right]} \qquad (1)$$

The ionic conductivity (σ) of PIL membrane were measured in the temperature of 5-60 °C via EIS measurements on a stainless steel|PIL|stainless steel battery under an amplitude of 5 mV in the frequency range of 0.1 - 10^5 Hz. σ was calculated from $\sigma = {}^{l_{(thickness\ of\ PIL,\ \ cm)}}\Big/ R_{b\ (bulk\ resistance,\ \ \Omega)} \times S_{(contact\ area,\ \ cm^2)}$

Theoretical calculations: All the geometry relaxations and electronic property calculations within density functional theory (DFT) were performed by using Quantum Espresso. [3] The Perdew-Burke-Ernzerhof functional within the generalized gradient approximation (PBE-GGA) was used to describe the electron exchange-correlation interaction. [4] The DFT-D3 method of Grimme [5] was used to describe long-range Van der Waals (vdW) interactions between Li (001) surface and

PEMEImTFSI. The energy cutoff for the plane-wave basis expansion and convergence threshold for energy was set to 80 Ry and 0.01 eV $Å^{-1}$, respectively. The Brillouin zone was sampled with a 3 × 3 × 1 k-point mesh. A vacuum of at least 16 Å in the z-direction was introduced to avoid the interaction between two periodic units.

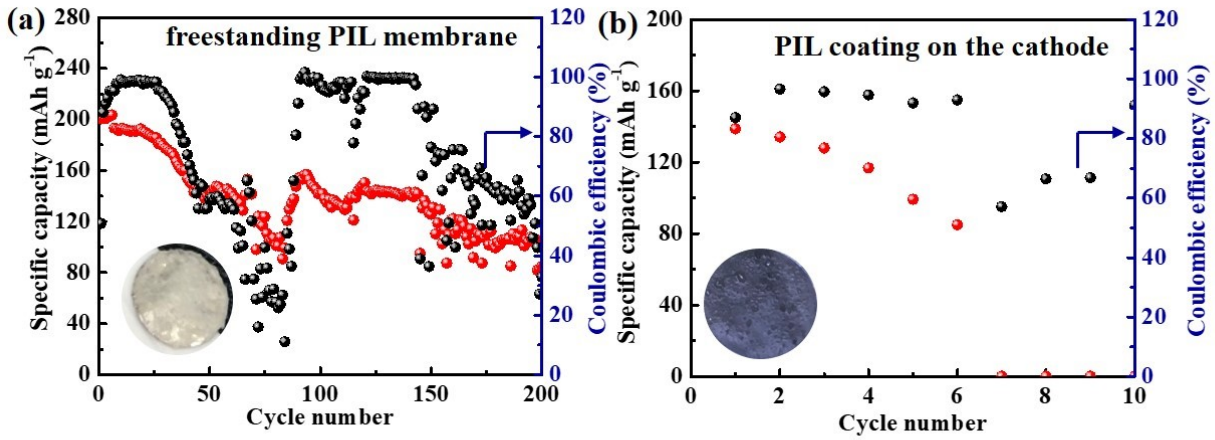

Fig. S1 Electrochemical performance of Li|$LiFePO_4$ batteries at 25 °C.

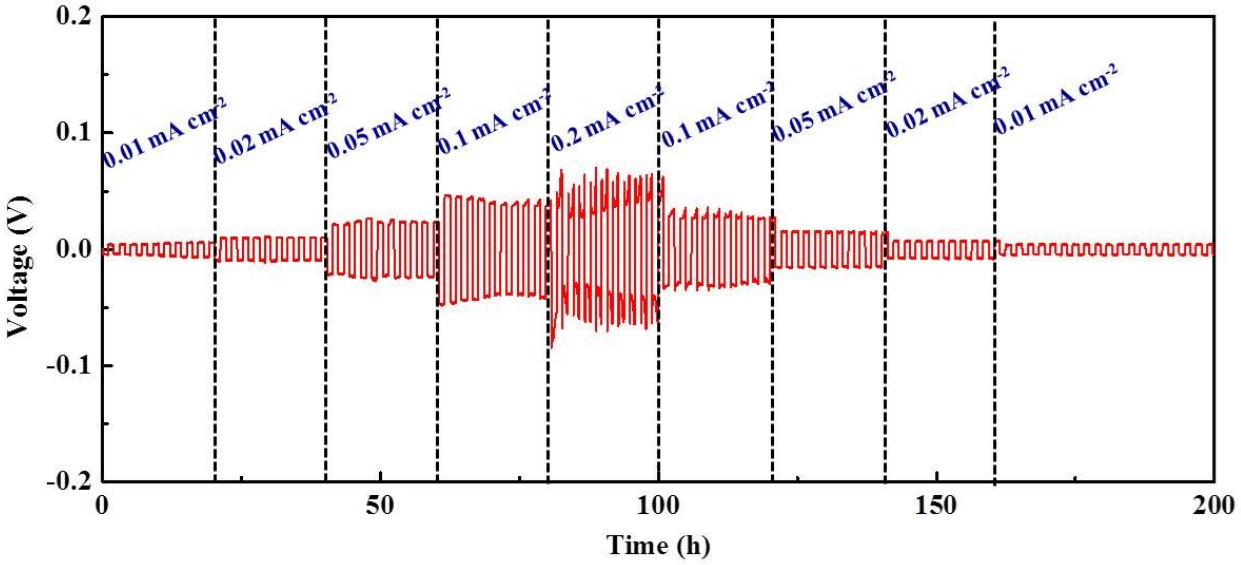

Fig. S2 Galvanostatic cycling profiles of Li|PIL|Li batteries at various current densities at room temperature.

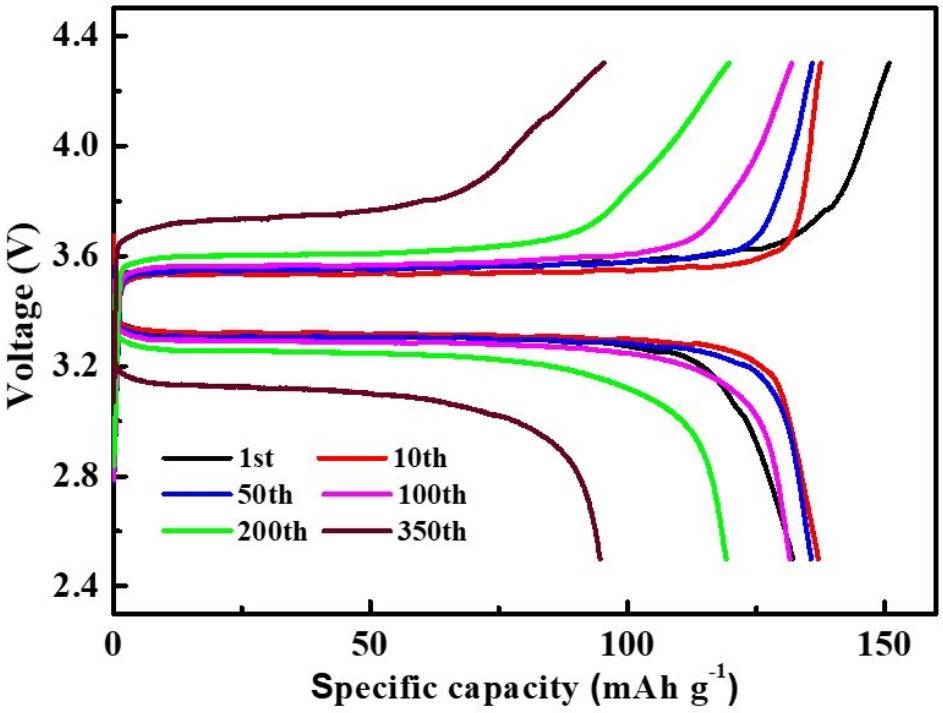

Fig. S3 Typical charge-discharge voltage profiles of Li|PIL|LFP batteries at 0.2 C and room temperature.

Table S1 Molecular weights of PIL polymers

Sample	M_w (Da)	M_n (Da)	M_w/M_n
PIL-1	15209	10196	1.492
PIL-2	28418	22473	1.265
PIL-3	44188	24177	1.828

Table S2 Electrochemical performance of polymer electrolytes consisting of PMMA/EMIMTFSI

PMMA	EMIMTFSI	LiTFSI	Electrochemical performance
1	1	2 M	Short circuit (on the anode)
1	1/2	2 M	No working (on the anode)
1	1/5	2 M	No working (on the anode)
1	1/10	2 M	Free-standing membrane (decaying shortly)

Table S3 Performance of different solid electrolyte materials

Solid electrolyte	Thermal stability	Electrochemical window	Ionic conductivity/ $\times 10^{-4}$ S cm^{-1}	t_{Li+}	Chemical compatibility towards Li anodes	Difficulty in device integration	Environmental friendliness	Mechanical properties	Cost
Li_6PS_5Cl [6]	/	/	120 at 25 ° C	/	unstable	high	unfriendly	High	High
$LiNbO_3$ doped Li_6PS_5Cl [7]	/	5 V	40.9 at 25 ° C	/	unstable	high	unfriendly	High	High
LAGP [8]	> 600	/	5.87 at 30 ° C	/	unstable	medium	friendly	High	High
LLZO/PVDF-HFP fiber network [9]	260 ° C	4.83 V	4.65 at 40 ° C	0.56	stable	low	relatively friendly	Medium	Medium
LATP-LiTFSI-Py_{13}TFSI-PDADMATFSI [10]	400 ° C	4.9 V	1.03 at 40 ° C	0.45	stable	low	relatively friendly	Medium	Low
TEOS in PAN [11]	324 ° C	5.2 V	4.3 at 20 ° C	0.52	stable	low	relatively friendly	Medium	Low
EMIm-TFSI in cross-linking EPVIm-TFSI/PEI/PVDF-HFP network [12]	340 ° C	5.0 V	18 at 25 ° C	0.33	stable	low	relatively friendly	Medium	Low
PEO networks crosslinked by imine and disulfide bonds [13]	356 ° C	>4.9 V	6.97 at 25 ° C	0.48	stable	low	relatively friendly	Medium	Low
PEO-$Pyr_{1,(2O)7}$TFSI-LiTFSI [14]	350 ° C	5.2 V	6.6 at 25 ° C	0.10 ± 0.01	stable	low	relatively friendly	Medium	Low
crosslinked PEGDE [15]	259 ° C	4.5 V	0.89 at 25 ° C	/	stable	low	relatively friendly	Medium	Low
EMIMTFSI/P(MMA-co-AMIMTFSI) [16]	260 ° C	4.6 V	1.9 at 25 ° C	0.17	stable	low	relatively friendly	Medium	Low
SnF_2 catalyzed P-DOL [17]	85 ° C	/	0.72 at 45 ° C	0.86	stable	low	relatively friendly	Medium	Low
PDADMAFSI-PYR_{13}FSI [18]	300 ° C	>5 V	8.0 at 25° C	0.44	stable	low	relatively friendly	Medium	Low
Our work	190 ° C	5.2 V	1.76 at 25° C	0.31	stable	low	relatively friendly	Medium	Low

References

[1] B.Yu, F. Zhou, C. W. Wang, W. M. Liu, *Eur. Polym. J.*, 2007, **43**, 2699-2707.

[2] S. J. Ding, H. D. Tang, M. Radosz, Y. Q. Shen, *Polym. Chem.*, 2004, **42**, 5794-5801.

[3] P. Giannozzi, S. Baroni, N. Bonini, M. Calandra, R. Car, C. Cavazzoni, D. Ceresoli, G. L. Chiarotti, M. Cococcioni, I. Dabo, et al. *J. Phys.: Condens. Matter*, 2009, **21**, 395502.

[4] J. P. Perdew, K. Burke, M. Ernzerhof, *Phys. Rev. Lett.*, 1996, **77**, 3865-3868.

[5] S. Grimme, S. Ehrlich, L. Goerigk, *J. Comput. Chem.*, 2011, **32**, 1456-1465.

[6] B.Yu, F. Zhou, C. W. Wang, W. M. Liu, *Eur. Polym. J.*, 2007, **43**, 2699-2707.

[7] S. J. Ding, H. D. Tang, M. Radosz, Y. Q. Shen, *Polym. Chem.*, 2004, **42**, 5794-5801.

[8] C. Y. Fu, G. Homann, R. Grissa, D. Rentsch, W. G. Zhao, T. Gouveia, A. Falgayrat, R. Y. Lin, S. Fantini, C. Battaglia, *Adv. Energy Mater.*, 2022, **12**, 2200412.

[9] Q. Liu, D. Zhu, D. Shanmukaraj, P. Li, F. Y. Kang, B. H. Li, M. Armand, G. X. Wang, *ACS Energy Lett.*, 2020, **5**, 1456-1464.

[10] J. Tan, J. Matz, P. Dong, J. F. Shen, M. X. Ye, *Adv. Energy Mater.*, 2021, **11**, 2100046.

[11] P. Jaumaux, Q. Liu, D. Zhang, X. F. Xu, T. Y. Wang, Y. Z. Wang, F. Y. Kang, B. H. Li, G. X. Wang, *Angew. Chem. Int. Ed.*, 2020, **59**, 9134-9143.

[12] C. Y. Chang, Y. Yao, R. R. Li, Z. H. Guo, L. W. Li, C. X. Pan, W. G. Hu, X. Pu, *Nano Energy*, 2022, **93**, 106871.

[13] Y. Cao, H. M. Lu, B. B. Xu, W. W. Yang, Q. S. Hong, *Chem. Eng. J.*, 2019, **378**, 122247.

[14] Y. Cao, H. M. Lu, Q. S. Hong, B. B. Xu, J. R. Wang, Y. Deng, W. W. Yang, W. Cai, *Carbon*, 2019, **144**, 280-288.

[15] W. W. Yang, H. M. Lu, Y. Cao, P. C. Jing, X. Q. Hu, H. Yu, *Ionics*, 2020, **26**, 3405-3413.

[16] W. W. Yang, H. M. Lu, Y. Cao, B. B. Xu, Y. Deng, W. Cai, *ACS Sustain. Chem. Eng.*, 2019, **7**, 4861-4867.

[17] J. X. Liu, Zhang, S. Q. Yuan, W. W. Yang, Y. Cao, J. Y. Deng, B. B. Xu, H. M. Lu, *Chem. Eng. J.*, 2022, **428**, 131326.

[18] Z. Li, J. L. Fu, S. Zheng, D. G. Li, X. Guo, *Small*, 2022, **18**, 2200891.